# Determination of atomic hydrogen in hydrocarbons by means of the reflected electron energy loss spectroscopy and the X-ray photoelectron spectroscopy

**V P Afanas'ev[1], A S Gryazev[1], D S Efremenko[2], P S Kaplya[1], O Y Ridzel[1]**

[1]National Research University "Moscow Power Engineering Institute", Department of General Physics and Nuclear Fusion, 14 Krasnokazarmennaya st., Moscow 111250, Russia
[2]Deutsches Zentrum für Luft- und Raumfahrt (DLR), Institut für Methodik der Fernerkundung (IMF), Oberpfaffenhofen 82234, Germany

Corresponding author e-mail: pavel@kaplya.com

**Abstract**. Elastic peaks electron spectroscopy (EPES) is a perspective tool for measuring the hydrogen atomic density in hydrocarbons. It is known that hydrogen elastic peaks overlap inelastic energy loss spectra. This fact complicates the quantitative interpretation of EPES spectra. In this paper, a novel technique based on the joint use of EPES and X-ray photoelectron spectroscopy (PES) is proposed. A key part of the method is the inelastic scattering background subtraction which is performed in two steps. At the first step, differential inelastic scattering cross-sections are retrieved from PES spectra, while at the second step, the retrieved cross-sections are used to remove the inelastic scattering signal from EPES spectra. Both REELS and PES spectra are described on the base of the invariant imbedding method forming a consistent framework for the surface state analysis. A good agreement is obtained between calculated spectra and experimental data.

## 1. Introduction

Hydrogen influences mechanical properties of construction materials. The studies of hydrogen storage in metals and plasma-material interactions in a fusion reactor require an efficient method for quantitative analysis of hydrogen isotopes. According to [1], methods based on the electron spectroscopy usually have problems with detecting hydrogen and helium. Nevertheless, recently several techniques have been proposed for measuring the bound hydrogen by means of electron spectroscopy [2–11]. A perspective tool for hydrogen detection is the elastic peak electron spectroscopy (EPES) [10, 12]. In the EPES, information on the sample composition is acquired from elastic energy losses (typically, in the range 0-20 eV) which are due to the elastic electron reflection. The amount of electron energy loss $\Delta E$ in a single elastic scattering event can be computed using the conservation laws for energy and momentum. The final expression reads:

$$\Delta E \cong \frac{2m}{M} E_0 (1 - \cos \psi) \qquad (1)$$

Here $m$ is the electron mass, $M$ is the scattering atom mass, $E_0$ is the initial electron energy and $\psi$ is the scattering angle. Elastically scattered electrons which have not experienced inelastic scattering

processes form a so-called "elastic peak" in the spectrum. The peak shape can be approximated by the Gaussian distribution [13] with full width at half maximum (FWHM) given by

$$2\sigma = 2\sqrt{\sigma_A^2 + \sigma_B^2 + \sigma_D^2} \tag{2}$$

where $\sigma_A$ is the broadening due to the energy analyzer slit function, $\sigma_B$ is the broadening of the electron beam, $\sigma_D$ is the Doppler broadening. The Rayleigh criterion for two peaks with maximums at $E_1$ and $E_2$ to be distinguished reads as $|E_1 - E_2| \geq \sigma$. From (1) it follows that the hydrogen atoms with the lowest atomic mass possible have the largest elastic peak shift. Therefore, elastic peaks corresponding to hydrogen isotopes can be easily resolved on the state-of-the-art setups. However, the hydrogen elastic peak overlaps with the inelastic scattering losses. This complicates conducting analysis of EPES data.

In this paper, we propose a method for the inelastic scattering background subtraction from EPES spectra. This method is based on the joint analysis of the photoelectron spectra (PES) and REELS spectra. Essentially, any mathematically justified technique of the background subtraction has to utilize information on the differential inverse inelastic mean free path (DIIMFP):

$$\omega_{in}(\Delta) = \frac{d\sigma_{in}}{d\Delta} \tag{3}$$

where $\sigma_{in} = (nl_{in})^{-1}$ is the inelastic electron scattering cross-section and $l_{in}$ is the inelastic mean free path (IMFP). Therefore, the background subtraction is performed in two steps. At the first step, differential inelastic scattering cross-sections are retrieved from PES spectra, while at the second step, the retrieved cross-sections are used to remove the inelastic scattering signal from EPES spectra.

## 2. Theoretical

### 2.1. General considerations

We consider the hydrocarbon surface samples that has been prepared in the Max Planck Institute of Plasma Physics (Max-Planck-Institut für Plasmaphysik, IPP) on the plasma-chemical sputtering setup [10]. The samples are investigated using the experimental setup NanoFab 25 at the National Research University «MPEI». The initial analysis is performed using the XPS method. The corresponding PES spectrum is shown in figure 1. Apparently, the sample is quite clean since almost only those peaks that correspond to O and C are seen in the spectrum. Note, that the spectrum contains a background, which is due to inelastic scattering events (plasmon excitations and ionization of the inner electron shells).
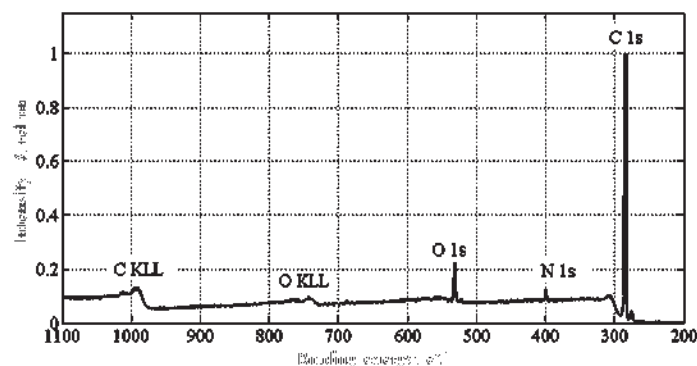


**Figure 1.** The PES spectrum for the hydrocarbon: excitation is done using the nonmonochromatic Mg K$_\alpha$ X-ray source.

Given the initial electron energy of 3 keV, the value of energy losses after one elastic scattering collision by a hydrogen atom according to Eq. (1) equals to 4.88 eV. Essentially, $\omega_{in}(\Delta)$ is nonmonotonic function with the first maximum in the region 10-20 eV. In the region 5-10 eV, $\omega_{in}(\Delta)$ increases with $\Delta$ and provide the signal comparable to the elastic peaks. The shape of $\omega_{in}(\Delta)$ which is referred to as a normalized differential inverse inelastic mean free path (NDIIMFP) is given by

$$x_{in}(\Delta) = \frac{\omega_{in}(\Delta)}{\sigma_{in}}, \quad \int_0^{E_0} x_{in}(\Delta)d\Delta = 1 \tag{4}$$

Below, we describe an algorithm for NDIIMFP retrieval from PES spectra.

### 2.2. Accounting for multiple scattering

Mathematically, the NDIIMFP retrieval problem is a deconvolution problem. To perform the deconvolution, we have to map the single scattering signal to the multiple scattering signal. To account for the impact of multiple scattering collisions, we adopt the formalism of Ambartsumian-Chandrasekhar equations. Let us introduce functions $Q_k$, $R_k$ which are the photo-electron flux density function and the reflection function of particles that have experienced exactly $k$ inelastic scattering events, respectively. Then, in the wide range of energy losses the functions $Q$ and $R$ are expanded in series of $Q_k$- and $R_k$-functions, respectively:

$$Q(\Delta, \mu_0, \mu, \varphi) = Q_0(\mu_0, \mu, \varphi)\delta(\Delta) + \sum_{k=1}^{\infty}\left[Q_k(\mu_0, \mu, \varphi)x_{in}^k(\Delta)\right] \tag{5}$$

$$R(\Delta, \mu_0, \mu, \varphi) = R_0(\mu_0, \mu, \varphi)\delta(\Delta) + \sum_{k=1}^{\infty}\left[R_k(\mu_0, \mu, \varphi)x_{in}^k(\Delta)\right] \tag{6}$$

$$x_{in}^1(\Delta) = x_{in}(\Delta), \quad x_{in}^{k+1}(\Delta) = \int_0^{\Delta} x_{in}^k(\Delta-\varepsilon)x_{in}(\varepsilon)d\varepsilon \tag{7}$$

Here $Q_k$ and $R_k$ correspond to $k$-fold inelastically scattered particles. If $x_{in}(\Delta)$ stands for the energy spectrum, which is observed after a single inelastic scattering event, then the $k$-fold convolution $x_{in}^k(\Delta)$ identifies the energy loss spectrum after $k$ successive inelastic scattering events. Essentially, $Q_k(\mu_0, \mu, \varphi)$ can be found only together with $R_k(\mu_0, \mu, \varphi)$. The equations for $Q_k(\mu_0, \mu, \varphi)$ and $R_k(\mu_0, \mu, \varphi)$ obtained using the invariant imbedding method are given in [14, 15]. The derivation consists in adding a layer of thickness $d\tau$ above the $\tau$-thickness layer and finding corresponding changes in $Q_k$ and $R_k$. The value of $d\tau$ is assumed to be small enough to neglect multiple scattering processes in this layer. The equation for $Q_k(\mu_0, \mu, \varphi)$ for a semi-infinite layer is given by [14, 16]

$$\frac{1}{\mu}Q_k(\mu_0, \mu, \varphi) - (1-\delta_{k0})\frac{1-\lambda}{\mu}Q_{k-1}(\mu_0, \mu, \varphi) = \delta_{k0}\lambda_\gamma f(\mu_0, \mu, \varphi)$$
$$+ \lambda_\gamma f \otimes R_k + \lambda Q_k \otimes x_{el} + \lambda Q_k \otimes x_{el} \otimes R_0 + \lambda \sum_{j=0}^{k-1} Q_j \otimes x_{el} \otimes R_{k-j} \tag{8}$$

Here $\lambda = \dfrac{\sigma_{el}}{\sigma_{el}+\sigma_{in}}$, $\lambda_\gamma = \dfrac{\sigma_\gamma}{\sigma_{el}+\sigma_{in}}$, $\sigma_{el}$ is the total elastic cross-section [17] and $\sigma_\gamma$ is the total photo-ionization cross-section [18]. The values of $l_{in}$ are taken from [19].

The equation for $R_k(\mu_0, \mu, \varphi)$ for a semi-infinite layer was considered in [15]. It reads:

$$\left(\frac{1}{\mu}+\frac{1}{\mu_0}\right)R_k = \lambda x_{el}\delta_{k0} + \lambda x_{el}\otimes R_k + \lambda R_k \otimes x_{el} + \lambda R_0 \otimes x_{el}\otimes R_k$$
$$+\lambda R_k \otimes x_{el}\otimes R_0 + \lambda\sum_{j=1}^{k-1} R_j \otimes x_{el}\otimes R_{k-j} + (1-\lambda)\left(\frac{1}{\mu}+\frac{1}{\mu_0}\right)R_{k-1} \tag{9}$$

In the context of Eqs. (8) and (9), the samples are assumed to be homogeneous, which implies that the difference between surface and bulk scattering properties is neglected. Further, the NDIIMFP is approximated as follows:

$$x_{in}(\Delta) = \sum_{i=1}^{N_{pl}}\lambda_{pl\,i}x_{pl\,i}(\Delta) + \sum_{j=1}^{N_{ion}}\lambda_{ion\,j}x_{ion\,j}(\Delta)$$
$$x_{pl\,i}(\Delta) = \frac{A_{pl\,i}\Delta^{\beta}}{\left(\Delta^2-\varepsilon_{pl\,i}^2\right)^2+\Delta^{\alpha}b_i^{4-\alpha}}, \quad x_{ion\,j}(\Delta) = \frac{A_{ion\,j}}{\Delta^2}\eta\left(\Delta-J_{ion\,j}\right) \tag{10}$$

where $J_{ion\,j}$ is the ionization threshold and $\eta\left(\Delta-J_{ion\,j}\right)$ is the Heaviside step function for the ionization energy. The coefficients $A_{pl\,i}$ and $A_{ion\,j}$ are introduced here to fulfill the following normalization conditions:

$$\int_0^{E_0} x_{pl\,i}(\Delta)\,d\Delta = 1, \quad \int_0^{E_0} x_{ion\,j}(\Delta)\,d\Delta = 1$$

$$\sum_{i=1}^{N_{pl}}\lambda_{pl\,i} + \sum_{j=1}^{N_{ion}}\lambda_{ion\,j} = 1$$

Essentially, Eqs. (8) and (9) are Sylvester linear matrix equations, while Eq. (9) setting $k$=0 is the Ricatti matrix equation. These equations are discretized in the angular domain and solved numerically in the discrete ordinate space using standard mathematical packages. Note, that the computational time for solving Eqs. (8) and (9) does not exceed a second. Therefore, this technique can be efficiently used in the fitting procedure.

## 3. Results and discussion
To compare calculations to experimental data, the result from Eq. (5) should be convoluted with the slit function $G_Q(\varepsilon)$ as follows:

$$Q_{fit}(\Delta,\mu_0,\mu,\varphi) = \int_0^{\Delta} Q(\Delta-\varepsilon,\mu_0,\mu,\varphi)G_Q(\varepsilon)\,d\varepsilon \tag{11}$$
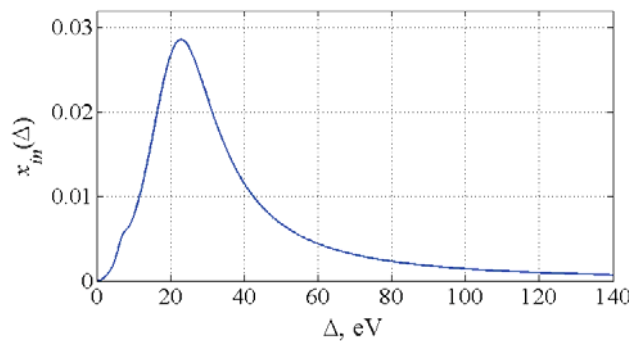


**Figure 2.** The NDIIMFP retrieved from the PES spectrum shown in figure 1.

The coefficients $\alpha$, $\beta$, $b_i$, $\varepsilon_{pl\ i}$, $J_{ion\ j}$ in Eq. (10) are found in the fitting procedure by minimizing the following objective function:

$$\gamma = \int_0^{\Delta_{max}} \left| Q_{exp}\left(\Delta,\mu_0,\mu,\varphi\right) - Q_{fit}\left(\Delta,\mu_0,\mu,\varphi\right) \right| d\Delta \tag{12}$$

where $(0, \Delta_{max})$ is the considered range of energy losses.

The comparison of the calculated spectrum using the retrieved NDIIMFP with the experimental spectrum is shown in figure 3, while the reconstructed NDIIMFP is presented in figure 2. The carbon oxide peak and the Mg $K_{\alpha3}$, Mg $K_{\alpha4}$ X-ray source satellite peaks are taken into account when computing $Q_{fit}$. The oxide peak in figure 3 is shifted from the main elastic peak by 3.6 eV. The relative intensities of the primary $\alpha_{1,2}$ and satellite $\alpha_3$, $\alpha_4$ X-ray peaks are given in Table 1. The corresponding data is taken from [1]. Given the reconstructed cross-section, the REELS spectrum $R\left(\Delta,\mu_0,\mu,\varphi\right)$ is computed and compared to the experimental data. The initial energy is 3 keV. Note, that just as for $Q\left(\Delta,\mu_0,\mu,\varphi\right)$, $R\left(\Delta,\mu_0,\mu,\varphi\right)$ should be convoluted with the slit function $G_R(\varepsilon)$ as follows:

$$R_{fit}\left(\Delta,\mu_0,\mu,\varphi\right) = \int_0^{\Delta} R\left(\Delta-\varepsilon,\mu_0,\mu,\varphi\right) G_R\left(\varepsilon\right) d\varepsilon \tag{13}$$

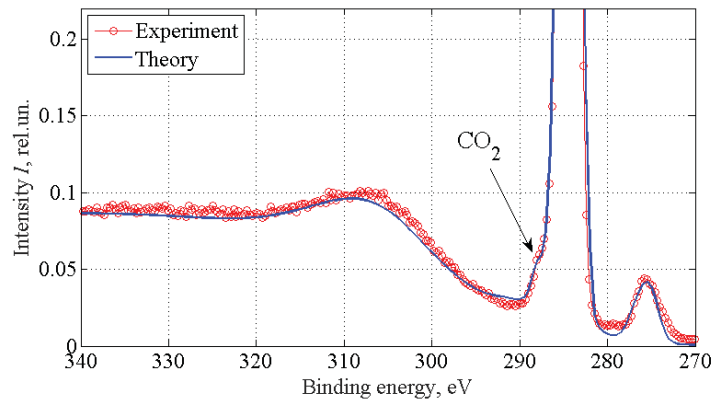The comparison is illustrated in figure 4.



**Figure 3.** The PES spectrum of the sample: excitation is done by using the nonmonochromatic Mg $K_\alpha$ X-ray source.

**Table 1.** X-ray satellite energies and intensities for Mg source.

|                          | $\alpha_{1,2}$ | $\alpha_3$ | $\alpha_4$ |
|--------------------------|---------------|-----------|-----------|
| **Rel. intensity (%)**   | 100           | 8.0       | 4.1       |
| **Energy displacement (eV)** | 0         | 8.4       | 10.2      |

The misfit between the experimental data and $R_{fit}\left(\Delta,\mu_0,\mu,\varphi\right)$ in the energy range of 2990÷2998 eV is due to the electron energy losses which occur during the elastic scattering collisions with hydrogen atoms. This effect in the context of EPES spectroscopy was quantitatively studied in [11, 13 20]. The FWHM of the EPES hydrogen peak agrees well with Eq. (2).
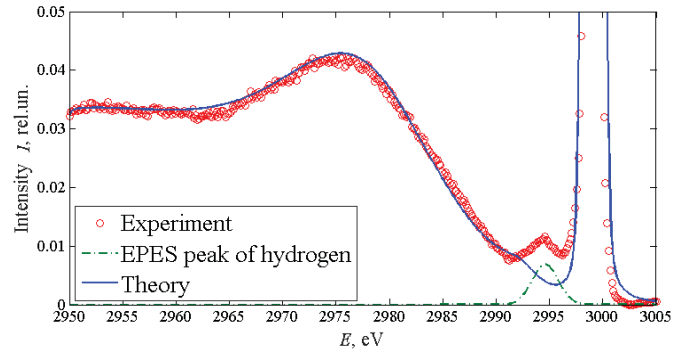
**Figure 4.** Comparison of the experimental data (circles) [10] and the calculated REELS spectrum using reconstructed cross-section (solid line). The dash-dot line corresponds to the retrieved EPES signal after subtracting the inelastic scattering background.

To perform a quantitative analysis, we assume that the investigated sample is homogeneous within a layer of thickness of $l_{in}$=6.5 nm, which corresponds to the EPES information depth [27]. With this assumption, we have a bijection between the elastic peak intensity and the quantity of the related element [21]. The fitting procedure gives the following ratio:

$$\frac{n_H}{n_C} = 1.3 \pm 0.1$$

Note, that this retrieved ratio is averaged in some sense over 10 nm layer from which the EPES signal originates from. Consequently, by varying the information depth our retrieval results can be refined and the depth resolution can be enhanced. In particular, in [10] the sample has been investigated using the nuclear reaction analysis (NRA) and the following ratio has been measured:

$$\frac{n_H}{n_C} = 0.53 \pm 0.04$$

This ratio is valid up to the depth of about 1 μm [22, 23]. Summarizing both results, we conclude that the amount of hydrogen is decreasing with the depth. For a more precise depth profiling, several EPES spectra measured at several initial energies $E_0$ (providing different information depths) can be incorporated in the presented algorithm.

## 4. Conclusion

The quantitative composition analysis of solids can be performed by using the elastic peak electron spectroscopy [3, 21]. The intensity of the elastic peaks depends on the concentration depth profile of a certain element [24]. In this paper, we proposed a method for the inelastic scattering background removal. This method is based on the joint interpretation of the REELS and PES spectra using the same NDIIMFPs retrieved from PES spectra. The background subtraction is performed in two steps. At the first step, differential inelastic scattering cross-sections are retrieved from PES spectra, while at the second step, the retrieved cross-sections are used to remove the inelastic scattering signal from EPES spectra.

Good agreement is obtained between the experimental data and numerical computations using Eqs. (8) and (9). From this we can conclude that the physical model that has been used for derivation of these equations is valid. In particular, there is a controversy regarding the photoelectron energy losses due to so-called intrinsic plasmon excitations. In this paper, all computations of electron energy loss spectra have been performed without accounting for intrinsic plasmon excitations, while all

physically relevant processes such as ionization, plasmon excitation and elastic collisions are considered in the same manner both for REELS and PES. The absence of intrinsic excitations was stated also in [14, 25, 26] in the context of the similar investigation of Al, Si, Mg and Nb samples. The presented NDIIMFP reconstruction technique accompanied with numerical tools for simulating REELS spectra leads to a consistent elastic peak analysis. Unlike several techniques described in [9], the proposed methods can be implemented using just one experimental setup with both REELS and PES capabilities.

## References

[1]     Hofmann S 2013 *Auger- and X-Ray Photoelectron Spectroscopy in Materials Science (Springer Series in Surface Sciences* vol 49) (Berlin, Heidelberg: Springer Berlin Heidelberg)

[2]     Vos M 2001 *Phys. Rev.* A **65** 012703

[3]     Vos M 2002 *Ultramicroscopy* **92** 143

[4]     Vos M, Chatzidimitriou-Dreismann C, Abdul-Redah T and Mayers J 2005 *Nucl. Instrum. Methods Phys. Res., Sect. B* **227** 233

[5]     Sulyok A, Gergely G, Menyhard M, Toth J, Varga D, Kover L, Berenyi Z, Lesiak B and Kosinski A 2001 *Vacuum* **63** 371

[6]     Gergely G 2002 *Prog. Surf. Sci.* **71** 31

[7]     Orosz G, Gergely G, Menyhard M, Tóth J, Varga D, Lesiak B and Jablonski A 2004 *Surf. Sci.* **566-568** 544

[8]     Yubero F, Rico V J, Espinos J P, Cotrino J and Gonzalez-Elipe A R 2005 *Appl. Phys. Lett.* **87** 084101

[9]     Yubero F and Tokesi K 2009 *Appl. Phys. Lett.* **95** 084101

[10]    Kostanovskiy I, Afanas'ev V, Naujoks D and Mayer M 2015 *J. Electron. Spectrosc. Relat. Phenom.* **202** 22

[11]    Afanas'ev V P, Afanas'ev M V, Lisov A A and Lubenchenko A V 2009 *Tech.Phys.* **54** 1667

[12]    Vos M and Went M 2007 *J. Electron. Spectrosc. Relat. Phenom.* **155** 35

[13]    Afanas'ev V, Afanas'ev M, Lubenchenko A, Batrakov A, Efremenko D and Vos M 2010 *J. Electron. Spectrosc. Relat. Phenom.* **177** 35

[14]    Afanas'ev V, Golovina O, Gryazev A, Efremenko D and Kaplya P 2015 *J. Vac. Sci. Technol. B* **33** 03D101

[15]    Afanas'ev V P and Kaplya P S 2015 *J.Surf.Invest.:X-ray, Synchrotron Neutron Tech.* **9** 715

[16]    Afanas'ev V, Kaplya P, Lubenchenko A and Lubenchenko O 2014 *Vacuum* **105** 96

[17]    Jablonski A, Salvat F and Powell C 2010 *NIST Electron Elastic-Scattering Cross-Section Database* – Version 3.2 (Gaithersburg, MD: National Institute of Standards and Technology)

[18]    Trzhaskovskaya M, Nefedov V and Yarzhemsky V 2001 *At. Data Nucl. Data Tables* **77** 97

[19]    Tanuma S, Powell C and Penn D 2011 *Surf. Interface Anal.* **43** 689

[20]    Afanas'ev V P, Afanas'ev M V, Batrakov A A, Bohmeyer W, Naujoks D, Lubenchenko A V and Markin A 2011 *J. Surf. Invest.: X-ray, Synchrotron Neutron Tech.* **5** 70

[21]    Afanas'ev V, Efremenko D and Lubenchenko A 2013 On the application of the invariant embedding method and RTE codes for surface state analysis *Light Scattering Reviews 8*, ed A A Kokhanovsky (Berlin, Heidelberg: Springer Berlin Heidelberg) chapter 8 pp 363

[22]    Ziegler J F and Biersack J P 1985 The stopping and range of ions in matter *Treatise on Heavy-Ion Science*, ed D Bromley (Boston, MA: Springer US) 93

[23]    Feldman L and Picraux S 1977 Selected low energy nuclear reaction data *Ion Beam Handbook for Material Analysis*, ed J Mayer and E Rimini (New York: Academic Press) chapter 4

[24]    Afanasyev V P, Efremenko D S, Lubenchenko A V, Vos M, Went M R 2010 *Bull. Russ. Acad. Sci.: Phys.* **74** 170

[25]    Afanas'ev V P, Gryazev A S, Kaplya P S, Andreyeva Y O, Golovina O Y 2016 *J. Surf. Invest.: X-ray, Synchrotron Neutron Tech.* **10** 101

[26]    Afanas'ev V P, Gryazev A S, Kaplya P S, Andreyeva Y O 2016 *J. Surf. Invest.: X-ray,*

*Synchrotron Neutron Tech.* **10** 113
[27]   Jablonski A, Powell C J 2004 *Surf. Sci.* **551** 106